Journal of Inflammation Research

Dovepress
Taylor & Francis Group

Open Access Full Text Article

ORIGINAL RESEARCH

Unveiling the Therapeutic Potential of Jiawei Jianpi Huoyu Formula in Ulcerative Colitis: A Multi-Strategies and Experimental Study Integrating Network Pharmacology, Machine Learning, and Mendelian Randomization

Xiaobei Lu[1], Yapeng Sun[2], Man Gong[1], Zhigang Sun[1], Xueru Fan[1], Na Huang[1], Liping Dai[1], Erping Xu[1]

[1]Traditional Chinese Medicine (Zhong Jing) School, Henan University of Chinese Medicine, Zhengzhou, 450046, People's Republic of China; [2]Third Affiliated Hospital of Henan University of Traditional Chinese Medicine, Zhengzhou, 450008, People's Republic of China

Correspondence: Erping Xu; Liping Dai, Henan Key Laboratory for Modern Research on Zhongjing's Herbal Formulae, Academy of Chinese Medical Sciences, Henan University of Chinese Medicine, 156 East Jinshui Road, Zhengzhou, 450046, People's Republic of China, Email xuerping@hactcm.edu.cn; liping_dai@hactcm.edu.cn

Background: Ulcerative colitis (UC) is a chronic inflammatory bowel disease. A modified traditional Chinese medicine (TCM) formula, "Jiawei Jianpi Huoyu Formula (JJHF)", has been reported to be effective in relieving UC symptoms, but its potential pharmacological components and targets remain unclear.

Methods: This study employs an integrative approach combining network pharmacology, machine learning, molecular docking, Mendelian randomization (MR), and experimental validation to investigate the therapeutic mechanisms of JJHF in UC.

Results: We identified 199 intersecting targets that were considered potential JJHF targets for treating UC. Network analysis revealed quercetin, luteolin, and kaempferol as key components modulating inflammatory pathways such as TNF and IL-6. Machine learning identified four core targets associated with UC progression, including glycogen synthase kinase 3 beta (GSK3B), vascular cell adhesion protein 1 (VCAM1), caspase-1 (CASP1), and heat shock protein family A member 5 (HSPA5). Molecular docking confirmed strong binding affinities between these targets and JJHF components, particularly β-sitosterol and HSPA5. In vitro experiments demonstrated that JJHF's efficacy in reducing LPS-induced inflammatory cytokines (IL-1β, TNF-α, MCP-1) and downregulating the expression of HSPA5, GSK3B, VCAM1, and CASP1 mRNA expression in RAW264.7 macrophages. In vivo, sixty mice were utilized to assess the efficacy of JJHF in DSS-induced colitis, where the JJHF alleviated colitis, improved colon length, disease activity index (DAI), and histopathology while suppressing pro-inflammatory cytokines. Notably, MR analysis established a causal link between elevated HSPA5 expression and UC risk (OR=5.639, p=0.040).

Conclusion: These findings highlight the innovative application of MR in JJHF research and underscore its multi-component, multi-target mechanisms in UC treatment, particularly through anti-inflammatory pathways and modulation of HSPA5 signaling. This study lays a scientific foundation for the clinical application and mechanistic exploration of JJHF in managing UC, offering potential advantages over standard therapies like mesalazine.

Keywords: Jiawei Jianpi Huoyu Formula, ulcerative colitis, network pharmacology, machine learning, Mendelian randomization analysis

Introduction

Ulcerative colitis (UC) is a chronic inflammatory condition that affects the gastrointestinal tract, causing recurrent inflammation and ulceration in the colon's mucosa.[1] An estimated 5 million cases of UC were reported globally in 2023, with a rising incidence rate worldwide.[2] Even with thorough research, the precise cause of UC is not fully understood. It

Received: 18 April 2025
Accepted: 11 July 2025
Published: 12 August 2025

Graphical Abstract

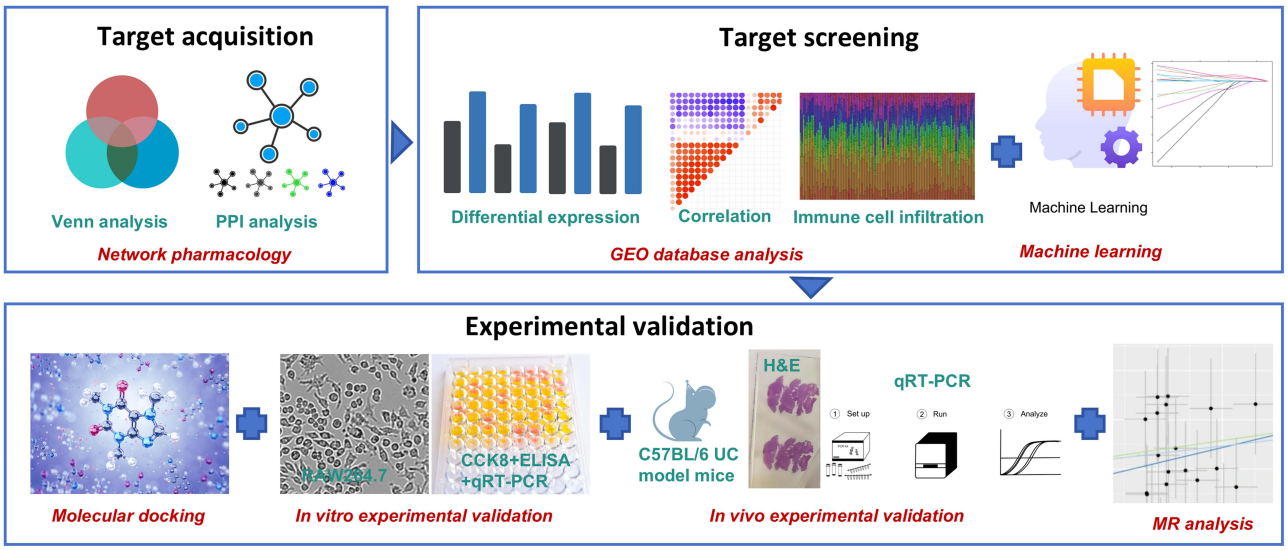

is clear that genetic and environmental factors, alongside emerging pathogenic elements like the melanocortin system, play a significant role in its development.[3,4] Currently, clinical treatments for UC include mainly pharmacological treatments (eg, aminosalicylates, corticosteroids, immunosuppressants, biologics, small molecules, and nanoagents[5,6]), which have become integral to the therapeutic landscape of UC. Although these treatments can be effective in controlling the symptoms of patients with UC to some extent, they are likely to be accompanied by certain side effects such as increased risk of infections and cancer.[7,8] Therefore, exploring more effective alternative complementary therapies is crucial to improve the symptoms of UC patients.

Traditional Chinese Medicine (TCM) offers a rich repository of herbal formulations that have been used to treat UC.[9,10] Our group has more than 30 years of clinical research foundation in Chinese medicine treatment of digestive system diseases. In the early stage, on the basis of the inheritance of the academic thought of Professor Li Zhenhua, a master of national medicine, and the summary of the famous veteran Chinese medicine practitioner, Professor Xu Erping, who combined with many years of clinical practice, proposed that spleen deficiency and blood stasis is the constant of the pathogenesis of UC, and strengthening the spleen and activating the blood stasis is the important law of the treatment of UC. Different from other TCM formulations that may focus solely on clearing heat, removing dampness, or tonifying the spleen, JJHF adheres to the principle of "strengthening the spleen and activating blood stasis" as the fundamental treatment strategy. The Jiawei Jianpi Huoyu Formula (JJHF) is a modified blend of the classic TCM formula Xiangsha Liujunzi Decoction from Yifang Jijie by Ang Wang in the Qing Dynasty. It is composed of *Radix Codonopsis Pilosulae* (Dangshen, 15 g), *Rhizoma Atractylodis Macrocephalae* (Baizhu, 20 g), *IIndian Buead Tuckahoe* (Fuling, 20 g), *Pinelliae Rhizoma* (Banxia, 10 g), *Amomi Fructus* (Sharen, 10 g), *Citri Reticulatae Pericarpium* (Chenpi, 10 g), *Cyperi Rhizoma* (Xiangfu, 15 g), *Curcumae Rhizoma* (Ezhu, 15 g), *Coicis Semen* (Yiyiren, 30 g), *Astragali Radix* (Huangqi, 25 g), *Notoginseng Radix* (Sanqi, 3 g), *Glycyrrhizae Radix et Rhizoma* (Gancao, 6 g), and *Bletillae Rhizoma* (Baiji, 20 g), JJHF comprehensively exerts the effects of invigorating the spleen, promoting blood circulation, and removing blood stasis. Clinical applications have demonstrated JJHF's promise in managing inflammatory bowel diseases, including UC. However, the mechanistic bases underlying the therapeutic effects of JJHF remain poorly defined.

Recent advances in systems pharmacological strategies have enabled the integration of multi-scale datasets including genomic, proteomic, and pharmacological data, offering new avenues to elucidate the effects of complex herbal formulations.[11–13] Indeed, by mapping the network interactions and pathways modulated by the JJHF in UC, our study could uncover novel therapeutic targets and mechanisms not observable when viewing components in isolation. Mendelian

randomization (MR) is a statistical method that uses genetic variation as an instrumental variable to study causal relationships between exposure factors and disease outcomes. By examining the impact of genetic variants (typically single nucleotide polymorphisms, SNPs) linked to exposure factors on disease, MR deduces the causal influence of exposure factors on disease.[14,15] So, in this study, we used an integrated approach to investigate the pharmacological effects of JJHF on UC by combining network pharmacology, machine learning, molecular docking, Mendelian randomization, and in vitro and in vivo experimental validation. This research not only clarifies the specific mechanisms by which JJHF alleviates symptoms of UC, but also provided a scientific foundation for promoting its clinical application.

Methods

Constituents and Related Targets in JJHF Formula

In order to identify the active components and their respective targets within the JJHF from the Traditional Chinese Medicine Systems Pharmacology Database and Analysis Platform (TCMSP), a screening criteria of oral bioavailability (OB) ≥ 30% and drug-likeness (DL) ≥ 0.18 was used. The herbs in JJHF consist of Radix Codonopsis Pilosulae (Dangshen), Rhizoma Atractylodis Macrocephalae (Baizhu), etc. Upon identifying the active compounds and their targets, the UniProt database (https://www.uniprot.org/) was used to correct gene names of the targets obtained from the TCMSP database. After the removal of duplicates, a final list of active compound targets was generated. Subsequently, comprehensive target information from the TCMSP database was collated and redundant entries were removed to yield the definitive list of pharmacological targets in this study on the JJHF.

Relevant Targets in UC

The genes related to UC were sourced from the GeneCards and CTD databases by searching the keyword "ulcerative colitis". The data retrieved from these databases were organized, filtered, and ultimately designated as targets for UC.

Construction of "Drug-Component-Target-Disease" Networks

The Venny online tool (https://bioinfogp.cnb.csic.es/tools/venny/) was used to discover common targets for JJHF and UC, which were then chosen as potential therapeutic targets for treating UC with JJHF. After that, Cytoscape 3.9.0 was used to construct a network showing the relationships between disease, drug, component, and targets, and a topological analysis was carried out to identify crucial components within the network.

Construction of Protein-Protein Interaction (PPI) Network

The intersection targets identified in Construction of "Drug-Component-Target-Disease" Networks were imported into the STRING database (https://cn.string-db.org/) and filtered with a minimum required interaction score of ≥ 0.4. The PPI network diagrams and TSV files were subsequently downloaded and saved. The PPI network was visualized using Cytoscape software (version 3.9.0). Subsequently, the PPI network was analyzed through clustering with the MCODE plug-in to identify the MCODE targets for treating UC with JJHF added.

GEO Sample Collection and Pre-Processing

In the GEO database, we looked for samples related to UC by using "ulcerative colitis" as the keyword. We specifically selected array expression profiles as the data type and "Homo sapiens" as the species, retrieving the GSE87466 dataset built upon the GPL13158 [HT_HG-U133_Plus_PM] Affymetrix array. This dataset comprises 87 UC patient samples and 21 normal controls, serving as the primary dataset for our analysis. We collected the gene expression matrix and clinical grouping information. To ensure statistical comparability across groups, the transcriptomic data were normalized using standard procedures: log2 transformation and quantile normalization were performed via the limma package in R to correct for technical variation. Next, we used Perl code to annotate gene symbols and correct data to obtain the MCODE gene expression levels of JJHF for UC in the samples from both normal and UC groups in network pharmacology.

Differential Expression of MCODE Genes, Chromosomal Location and Correlation of Core Gene Expression

Using the R software packages "limma", "heatmap", and "ggpubr", we analyzed the expression of MCODE genes in both normal subjects and UC patients. Genes with $P<0.05$ were considered for the core genes selection, and the differentially expressed MCODE genes were displayed in box plots and heatmaps. After identifying the core genes using Perl coding, we created a loop diagram for visual presentation. The core gene association coefficients were subsequently visualized and examined through the use of the R package "Rcircos".

Analysis of Immune Cell Infiltration in UC Patient Samples

1000 simulation experiments were performed on different immune cells using the "CIBERSORT" package of R software. These simulations not only provide precise data on the relative content of immune cells, but also establish a standard for quantifying the number of immune cells. For in-depth analysis of the differences in immune cells, we applied the R packages "GSVA" and "GSABase". These packages facilitated the use of the single-sample Gene Set Enrichment Analysis (ssGSEA) method, allowing us to compare the variances in immune cell content between the healthy control group and the UC patient group. Subsequently, to further examine and validate the core genes we identified, we performed correlation tests between the core genes and ssGSEA scores, followed by visualization of the correlation coefficients.

Selection of Machine Learning Models and Graphs for the Treatment of UC with the Addition of JJHF

Three machine learning algorithms (SVM-RFE, LASSO, and RF) were utilized to screen key genes among the significantly differentially expressed core genes in this study. Diagnostic markers for UC were categorized using Support Vector Machine (SVM) operator, Least Absolute Shrinkage and Selection Operator (LASSO), and Random Forest Algorithm (RF).[16] A 10-fold cross-validation was carried out using the "glmnet" package to distinguish between UC patients and healthy controls. To prevent overfitting, the SVM-RFE algorithm was used with the "e1071" and "svmRadial" packages to pinpoint high-quality genes. The RF classification model was built using the "randomForest" package, and UC-related genes were ranked based on the Gini index to identify core genes with distinctive expression patterns. Subsequently, the key genes were determined by intersecting SVM-RFE, LASSO, and RF among the significantly differentially expressed core genes. Once the key genes were determined, nomogram models were created based on the key genes and their expression levels in the normal and UC groups to further evaluate the diagnostic potential of the model in distinguishing between the normal and UC groups.

Molecular Docking Validation

In previous research, we identified the core active ingredients and key genes in JJHF. Subsequently, we obtained the three-dimensional structures of these core active ingredients and key genes using methods such as PubChem (https://www.example.com) and the Protein Data Bank (PDB) (www.rcsb.org/). Based on this information, we pre-treated the target proteins and small molecules and made structural modifications using methods such as Auto Dock to resolve their binding sites with proteins and identify active pockets. Target proteins and small molecule compounds were then introduced into AutoDock Vina 1.1.2, and the docking sites' coordinates were set for verification. The results were then analyzed using heatmap analysis, and the selected small molecules were visualized using Pymol software.

In vitro Cellular Experiments

JJHF Preparation

The JJHF was prepared in the Pharmacy Department of the First Affiliated Hospital of Henan University of Traditional Chinese Medicine. The formula includes the following ingredients: *Radix Codonopsis Pilosulae* (Dangshen, 15 g), *Rhizoma Atractylodis Macrocephalae* (Baizhu, 20 g), *IIndian Buead Tuckahoe* (Fuling, 20 g), *Pinelliae Rhizoma* (Banxia, 10 g), *Amomi Fructus* (Sharen, 10 g), *Citri Reticulatae Pericarpium* (Chenpi, 10 g), *Cyperi Rhizoma* (Xiangfu, 15 g), *Curcumae Rhizoma* (Ezhu, 15 g), *Coicis Semen* (Yiyiren, 30 g), *Astragali Radix* (Huangqi, 25 g), *Notoginseng Radix* (Sanqi, 3 g), *Glycyrrhizae*

Radix et Rhizoma (Gancao, 6 g), and *Bletillae Rhizoma* (Baiji, 20 g). All ingredients used in JJHF are purchased from Jiangsu Tianjiang Traditional Chinese Medicine Clinic Co., Ltd. and comply with the quality standards of the Chinese Pharmacopoeia. The above herbs were re-suspended in pure water, homogenized using a vortex mixer (2000 rpm, 5 minutes) to form a homogeneous suspension, aliquoted, and stored at −20°C. Prior to use, the suspension is reconstituted in a 37°C water bath. The low, medium, and high-dose groups correspond to 0.5 times (3.75 g/kg/day), 1 times (7.5 g/kg/day), and 2 times (15 g/kg/day) of the adult clinical equivalent dose, respectively.

Preparation of Drug-Containing Serum, Experimental Grouping and Administration

Sixty SD rats, after acclimatisation feeding, were randomly divided into control group, JJHF low, medium and high dose group and mesalazine group. After 7 days of drug administration, rats in each group were anaesthetised with 20% Urethane. Blood samples were collected from the abdominal aorta, subjected to centrifugation at 3000 × g for 15 min at 4 °C, and the serum was heat-inactivated at 56 °C for 30 min. The samples were then filtered through a 0.22 μm membrane and stored at −80 °C for further analysis.

Cell Culture and CCK-8 Assay

RAW264.7 macrophage cells, obtained from the CAS Cell Bank (Shanghai, China), were cultured in a humidified environment with 5% CO_2 at 37°C in DMEM supplemented with 10% fetal bovine serum (FBS) and 1% penicillin-streptomycin. To assess the cytotoxic effects of sera from various treatment groups on these cells, a CCK-8 assay was performed. Initially, cells were seeded in 96-well plates at a density of 1×10^4 cells per well and incubated overnight for attachment. After 24 hours, the cells were treated with serial dilutions of collected sera from different experimental groups (blank, JJHF low, medium, high dose, and mesalazine) in triplicate. Following another 24 hours of incubation with the sera, 10 μL of CCK-8 reagent was added to each well, and the plates were incubated for an additional 2 hours at 37°C. Finally, the optical density at 450 nm was measured using a microplate reader.

ELISA Assay

To assess the expression levels of IL-1β, TNF-α, and MCP-1 in LPS-induced RAW 264.7 cells, an ELISA method was employed. Firstly, the experiment was divided into blank group, model group, JJHF low-dose group, medium-dose group, high-dose group and mesalazine group, and then RAW 264.7 cells were stimulated with LPS for 24 hours. After stimulation, the culture supernatants were collected and centrifuged to remove cellular debris. The concentrations of IL-1β, TNF-α, and MCP-1 were then measured using specific ELISA kits (Elabscience, Wuhan, China) according to the manufacturer's instructions.

qRT-PCR Analysis

To assess the effect of JJHF on the expression levels of key targets HSPA5, GSK3B, VCAM1 and CASP1 mRNA, qRT-PCR analysis was performed. After LPS stimulation of RAW 264.7, they were classified into blank, model, JJHF low, medium and high dose and mesalazine groups. Following a 24-hour treatment with the respective sera, total RNA was extracted from the cells using an RNA extraction kit according to the manufacturer's protocol. The purity and concentration of the RNA were assessed using a spectrophotometer. Subsequently, cDNA was synthesized from 1 μg of RNA using a reverse transcription kit. qRT-PCR was conducted using specific primers for HSPA5, GSK3B, VCAM1, and CASP1, along with a housekeeping gene (β-actin) as a control. The amplification was performed in a real-time PCR system, and the relative expression levels of the target genes were calculated using the $2^{-\Delta\Delta Ct}$ method. The primer sequences of all analyzed genes are listed in Supplementary Table 1.

In vivo Animal Experimental Validation

Animals

A total of 100 male C57BL/6 mice (20–25 g, aged 6–8 weeks) were obtained from Beijing Vital River Laboratory Animal Technology Co., Ltd. and housed in SPF conditions at the Animal Experiment Center of Henan University of Traditional Chinese Medicine. The housing environment was maintained at a temperature of 24 ± 2 °C, with a humidity of 50%-60%, on a 12 h light/dark cycle. Mice were given free access to food and water, and after a one-week acclimatization period, they were randomly assigned to experimental groups.

Experimental Design

After acclimatization, the mice were weighed and numbered. Based on the principle of weight balancing, 60 mice were selected and divided into six groups (n=10 per group): control group, model group, low-dose JJHF group, medium-dose JJHF group, high-dose JJHF group, and mesalazine group. Colitis was induced in the mice by administering a 3% dextran sulfate sodium (DSS) solution in drinking water for 7 days. During this period, water was withheld, and fresh DSS solution was provided daily. Mice in the normal group received only regular drinking water, while all mice had free access to food. General conditions of the mice were observed daily, and fecal occult blood tests were performed to assess mucosal integrity. On the 7th day of DSS treatment, the body weight and disease activity index (DAI) was evaluated daily. For the collection of colonic tissues, segments from the anus to the cecum were excised, and the length of the colon was measured using a ruler. The colon was then longitudinally opened and rinsed 2–3 times with pre-chilled PBS. Excess PBS was removed using filter paper, and the colon tissue was cut into four segments, which were designated for histopathological and molecular biological assessments.

DAI Score

The DAI was assessed daily using a scoring system based on three parameters: weight loss, stool consistency, and the presence of fecal occult blood. Mice were assigned a score of 0 to 4 for each parameter, with 0 indicating normal conditions and higher scores reflecting increasing severity. Weight loss was scored from 0 (normal), 1 (1–5%), 2 (6–10%), 3 (11–15%), and 4 (greater than 15% weight loss), and fecal consistency was scored as 0 (normal formed feces), 1 (soft but firm), 2 (soft), 3 (wet), and 4 (watery diarrhea). Fecal occult blood was categorized as absent (score 0–1) and positive (score 2–3 for occult blood and score 4 for blood in stool). The total DAI score for each mouse was calculated by summing the individual scores.

Colon Length Measurement

At the end of the experiment, the mice were euthanized, and the colon was excised. The length of the colon was measured using a ruler.

Fecal Occult Blood Test

Fecal samples were collected, and a fecal occult blood test was performed to evaluate mucosal integrity.

Histological Analysis

Colonic tissue samples were fixed in 10% formalin and embedded in paraffin. Sections (4 μm) were stained with hematoxylin and eosin (H&E) for histopathological examination. Inflammatory changes were assessed by a blinded pathologist.

Cytokine and Gene Expression Analysis

The whole blood was collected in 1.5 mL centrifuge tubes and allowed to stand for 2 hours. Subsequently, the samples were centrifuged at 4 °C at 3500 rpm for 15 min to obtain serum, which was stored at −80 °C for later analysis. The serum levels of TNF-α, IL-6, IL-1β, and MCP-1 were measured using ELISA kits. The mRNA expression of HSPA5, VCAM1, GSK3B, and CASP1 in colonic tissues was analyzed via qRT-PCR as described above. The primer sequences of all analyzed genes are listed in Supplementary Table 1.

MR Analysis of Key Genes and UCs

To better understand how key genes are related to the risk of UC, we utilized MR analysis in two datasets, a method particularly effective for studying causal relationships. Initially, we collected SNPs associated with exposure factors and UC outcomes from the Integrative Epidemiology Unit (IEU) database (https://gwas.mrcieu.ac.uk/). Using the "TwoSampleMR" package, we applied the inverse variance weighted (IVW) method to accurately assess the link between gene expression levels and UC risk. Furthermore, Cochran's Q statistic was used to test for heterogeneity in the IVW results. A P value of less than 0.05 was considered statistically significant for heterogeneity. Finally, to fully assess possible horizontal pleiotropy, we used MR-Egger regression and MR-PRESSO analysis. When P was below 0.05, the IVW results showed significant horizontal pleiotropy.

Statistical Analysis

The data were analyzed using GraphPad Prism (version: 9.2.0). The results are expressed as mean ± standard deviation (SD). One-way ANOVA was used to compare differences among the treatment groups, followed by post-hoc Tukey's test for multiple comparisons. A $p<0.05$ was considered statistically significant.

Result

Collection of Active Ingredients and Related Targets in JJHF and Acquisition of UC-Related Targets

We searched the TCMSP database to gather information on the active ingredients and associated targets of JJHF. After eliminating duplicates and excluding irrelevant data, we identified a total of 173 active ingredients and 285 associated targets. These included Radix Codonopsis Pilosulae, which had 10 active ingredients and 110 associated targets, Rhizoma Atractylodis Macrocephalae with 7 active ingredients and 19 associated targets, Indigo Naturalis with 15 active ingredients and 25 related targets, Pinelliae Rhizoma with 9 active ingredients and 99 related targets, Citri Reticulatae Pericarpium with 3 active ingredients and 69 related targets, Amomi Fructus with 6 active ingredients and 54 related targets, Cyperi Rhizoma with 17 active ingredients and 226 related targets, Curcumae Rhizoma with 3 active ingredients and 24 related targets, Coicis Semen with 7 active ingredients and 32 related targets, and Notoginseng Radix with 7 active ingredients and 188 related targets. Additionally, Glycyrrhizae Radix et Rhizoma had 92 active ingredients and 233 related targets, Astragali Radix had 20 active ingredients and 213 related targets, and Bletillae Rhizoma had 9 active ingredients and 27 related targets. By further exploring the Genecards and CTD databases, we obtained 5460 and 25199 relevant targets, respectively. Utilizing the Venny online platform, we conducted an intersection analysis of drug-related and disease targets, ultimately pinpointing 199 targets directly linked to both drugs and diseases (Figure 1A).

"Drug-Component-Target-Disease" Network Analysis and PPI Network Analysis

To further understand the potential relationship between the core components of JJHF and its targets and UC disease, the construction of the "drug-component-target-disease" network was conducted using Cytoscape software (version 3.9.0) (Figure 1B). The network consists of 370 nodes, including 157 active ingredient nodes, 199 target nodes, 13 Chinese medicine nodes, and 1 disease node, with 2149 edges. The topological parameters of the network were analyzed using the Network Analyzer plugin, with an average number of neighboring nodes being 11.616, network heterogeneity at 1.695, network density at 0.031, and network centrality at 0.511. Nodes with higher degree values in the network are considered core nodes, and the top active ingredients with high Degree values are: MOL000098 (quercetin, Degree=126), MOL000006 (luteolin, Degree=53), MOL000422 (kaempferol, Degree=49), MOL004328 (naringenin, Degree=35), MOL002714 (baicalein, Degree=30), MOL000354 (isorhamnetin, Degree=29), MOL005828 (nobiletin, Degree=28), MOL003896 (7-Methoxy-2-methyl isoflavone, Degree=27), MOL000392 (formononetin, Degree=27), MOL000358 (beta-sitosterol, Degree=24), etc. (Supplementary Table 2). JJHF may have effective components acting on UC disease with multiple points of action and strong interactions, playing a central hub role in the network. Additionally, multiple targets are simultaneously influenced by a single component with multiple characteristics, and multiple components can simultaneously interact with a single target. It can be seen that JJHF treats UC disease through multi-component and multi-target joint regulation.

To better understand the mechanism of action of JJHF in treating UC, we used a PPI network to explore the interactions among its intersecting targets. We constructed a PPI network of 199 intersecting targets using data from STRING and Cytoscape software, which consisted of 197 nodes and 5049 edges, with an average node degree of 51.259. Subsequently, we performed clustering on the PPI network using the MCODE plugin (k = 4) and obtained 2 cluster networks (Figure 1C). To identify the core cluster genes, we selected genes with a degree value ≥ 1.25 times the median in each cluster network as MCODE genes. A total of 62 targets were selected, which are now considered to be the main genes involved in treating UC with JJHF, including AKT1, TNF, IL6, TP53, IL1B, etc.

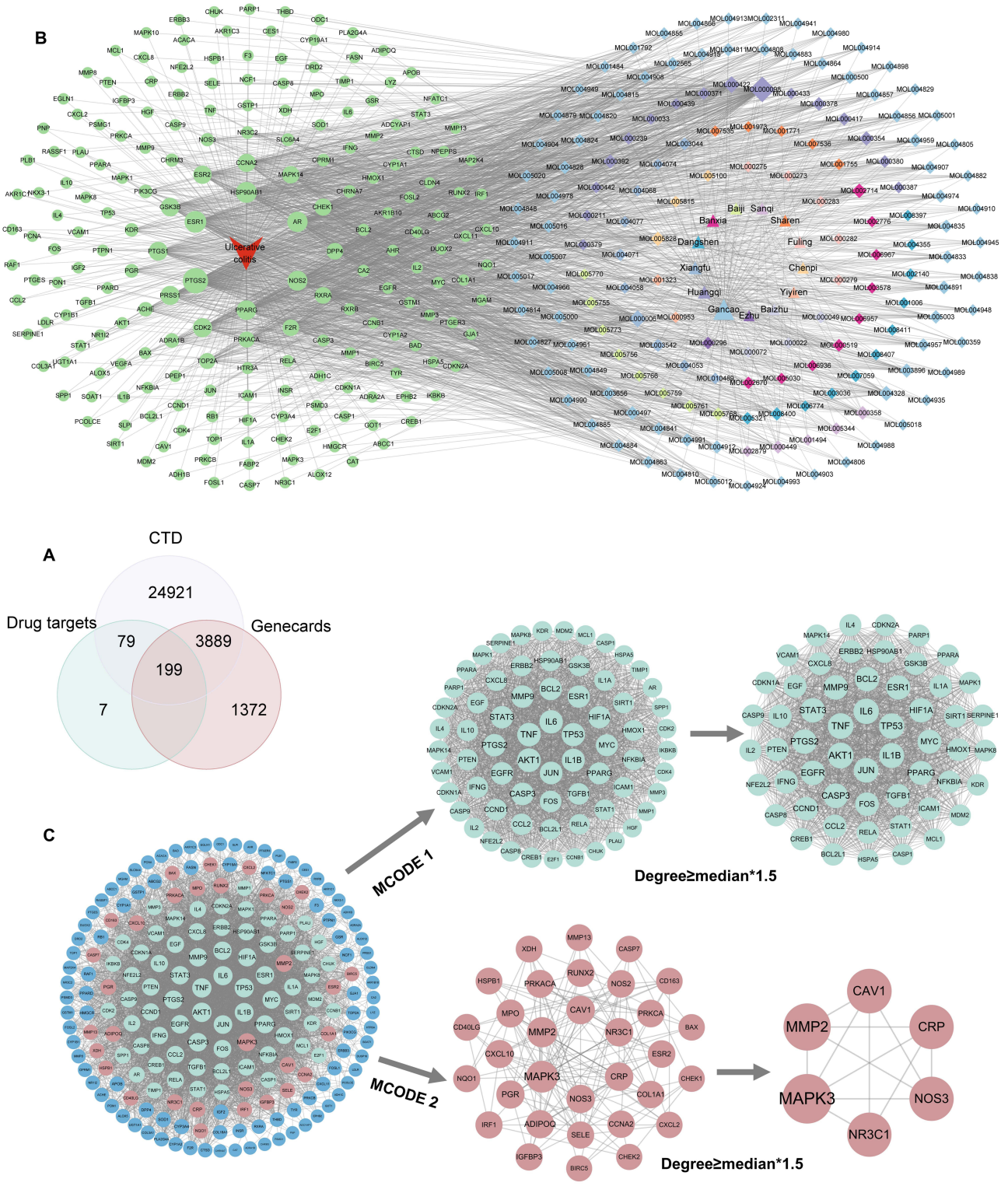

Figure 1 Network pharmacological analysis. (**A**) Venn diagram showing the intersection of drug targets and disease targets. (**B**) "Drug-ingredient-target-disease" network diagram. (**C**) Analysis of the PPI network with intersecting targets.

Acquisition of GEO Dataset Samples and MCODE Gene Correlation Analysis

Through web-based pharmacological analysis in JJHF, we identified 62 MCODE genes (Supplementary Table 3). Analysis of the GSE87466 dataset revealed that 46 core genes, such as TNF, IL6, IL1B, EGFR, PTGS2, STAT3, and MMP9, showed higher accuracy and clinical significance in distinguishing between UC and normal groups. With the exception of EGFR, BCL2, PPARG, and others which were highly expressed in the normal group, the UC group displayed elevated expression levels for the majority of genes (Figure 2A and B). The specific chromosomal locations of the core genes in JJHF are shown in Figure 2C. The correlation analysis of every two core genes in UC samples showed that the core genes were strongly correlated with each other, and the correlation was mainly positive (Figure 2D and E).

Analysis of Immune Cell Infiltration in Normal Samples and UC Samples

By linking the dynamics of immune cells with target gene regulation, we can better verify the anti-inflammatory mechanism of JJHF. Therefore, we carried out a detailed study of immune cell infiltration. This approach enabled us to precisely determine the types and proportions of immune cells present in each sample (Figure 2F). Moreover, ssGSEA analysis (Figure 2G) was conducted to pinpoint statistically significant immune cells in both the normal and UC groups. In the normal group, high expression levels were found for T cells CD8, Tregs, NK cells activated, T cells CD4 memory resting, Monocytes, Dendritic cells resting, Macrophages M2, and Mast cells resting. Conversely, the UC group exhibited high expressions of T cells CD4 memory activated, T cells gamma delta, T cells follicular helper, Macrophages M0, Dendritic cells activated, Macrophages M1, Mast cells activated, and Neutrophils. The immune cell correlation analysis (Figure 2H) demonstrated that certain immune cells were predominantly positively correlated with core genes. Of the immune cells significantly correlated ($P<0.05$) with core genes, Macrophages M0, Macrophages M1, and Neutrophils displayed primarily negative correlations.

Analysis of Machine Learning Models and Construction of UC Line Diagram Models

Our objective is to evaluate the diagnostic capabilities of core genes in differentiating between patients with UC and healthy individuals, considering their differences. By applying three machine learning algorithms (LASSO, SVM-RFE, and RF) to the UC dataset, we have identified important genes that can effectively differentiate UC patients from others. Within the SVM-RFE algorithm, we have identified 23 out of the 46 core genes as crucial targets (Figure 3A and B). In the LASSO algorithm, 12 genes were selected from the 46 intersection targets (Figure 3C and D). Additionally, based on the RF algorithm, 9 relevant genes were obtained by setting a screening criterion of importance greater than 1 for the 46 intersection genes (Figure 3E and F). Finally, combining the results of the three machine learning algorithms, four genes were identified as key genes, including GSK3B, VCAM1, CASP1 and HSPA5 (Figure 3G). Subsequently, to demonstrate the diagnostic potential of key genes in differentiating UC samples from healthy control samples, we constructed a column chart model of the key genes. The results showed that by calculating the sum of expression scores of these key genes, individual scores were plotted to determine treatment sensitivity and predict the risk rate of UC development based on the key genes (Figure 3H).

Validation of Molecular Docking

Based on the key target names obtained from the machine learning results, we downloaded the corresponding PDB files, namely: GSK3B (PDB ID: 2O5K), VCAM1 (PDB ID: 1VSC), CASP1 (PDB ID: 1BMQ), HSPA5 (PDB ID: 3LDL). After fully understanding the Degree parameter results in the "active ingredient-target" network, we selected the top ten active compounds: MOL000098 (quercetin), MOL000006 (luteolin), MOL000422 (kaempferol), MOL002714 (baicalein), MOL004328 (naringenin), MOL000354 (isorhamnetin), MOL005828 (nobiletin), MOL003896 (7-Methoxy-2-methyl isoflavone), MOL000392 (formononetin), MOL000358 (beta-sitosterol). The interaction strength between target proteins and active ingredients is represented by the docking score, where a negative binding energy value indicates a better binding affinity. A binding activity between the receptor protein and ligand small molecule is considered good when the binding energy is below −5 kcal/mol. A binding interaction is deemed strong when the binding energy is below −7 kcal/mol (Figure 4A–E).

https://doi.org/10.2147/JIR.S527482

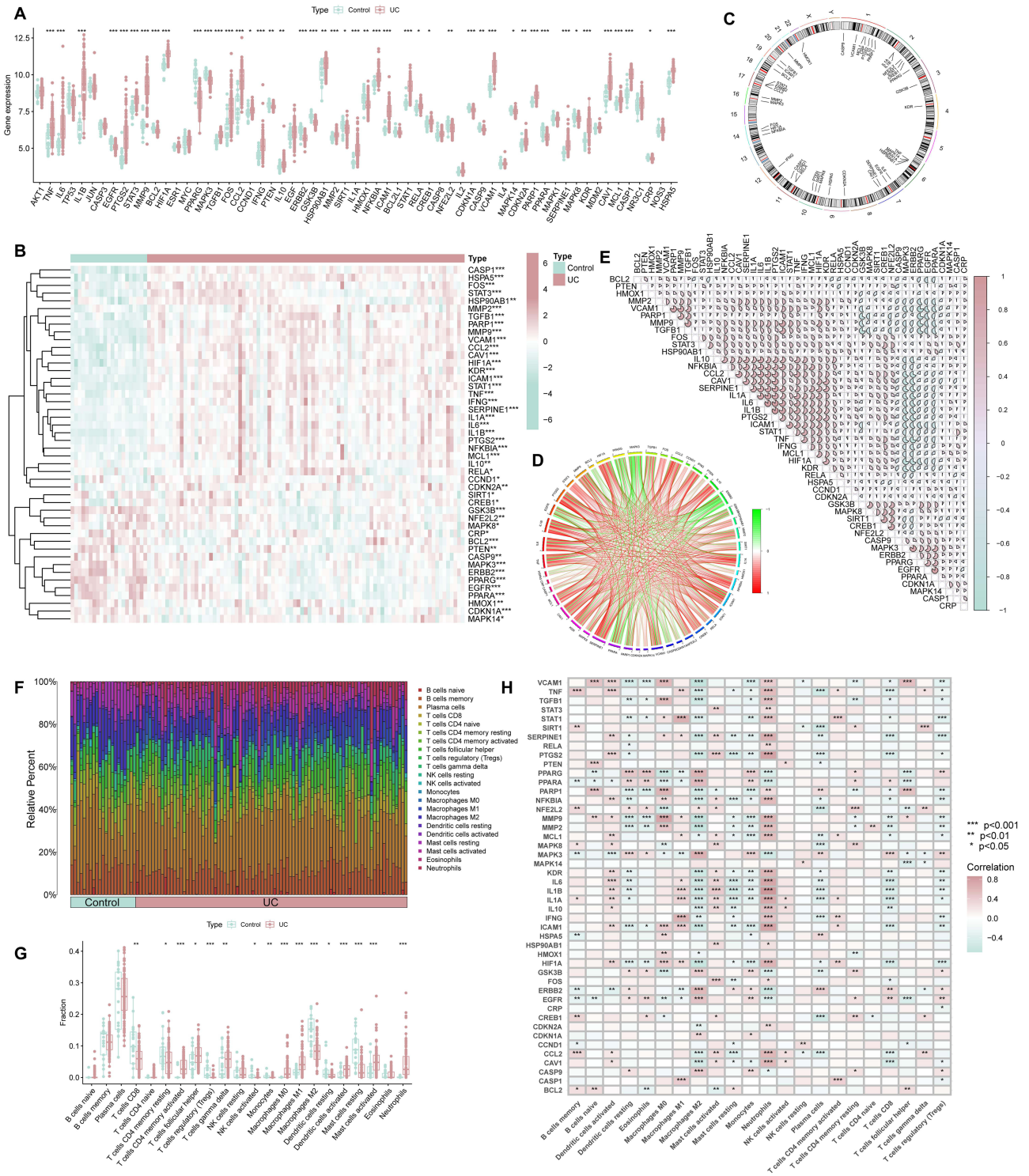

Figure 2 GEO dataset sample acquisition and analysis of MCODE gene correlation and immune cell infiltration. (**A**) Box plot analysis of differential gene expression between normal and UC samples. (**B**) Heat map of core gene expression in normal and UC samples. (**C**) Circular map of chromosomal locations of core genes. (**D**) Network analysis of core genes. (**E**) Correlation analysis graph between two core genes. (**F**) Bar graph of relative percentages of immune cells in samples. (**G**) Box plot of immune cell scores in normal and UC samples. (**H**) Heat map of correlation analysis between core genes and immune cells. * $p < 0.05$; ** $p < 0.01$; *** $p < 0.001$.

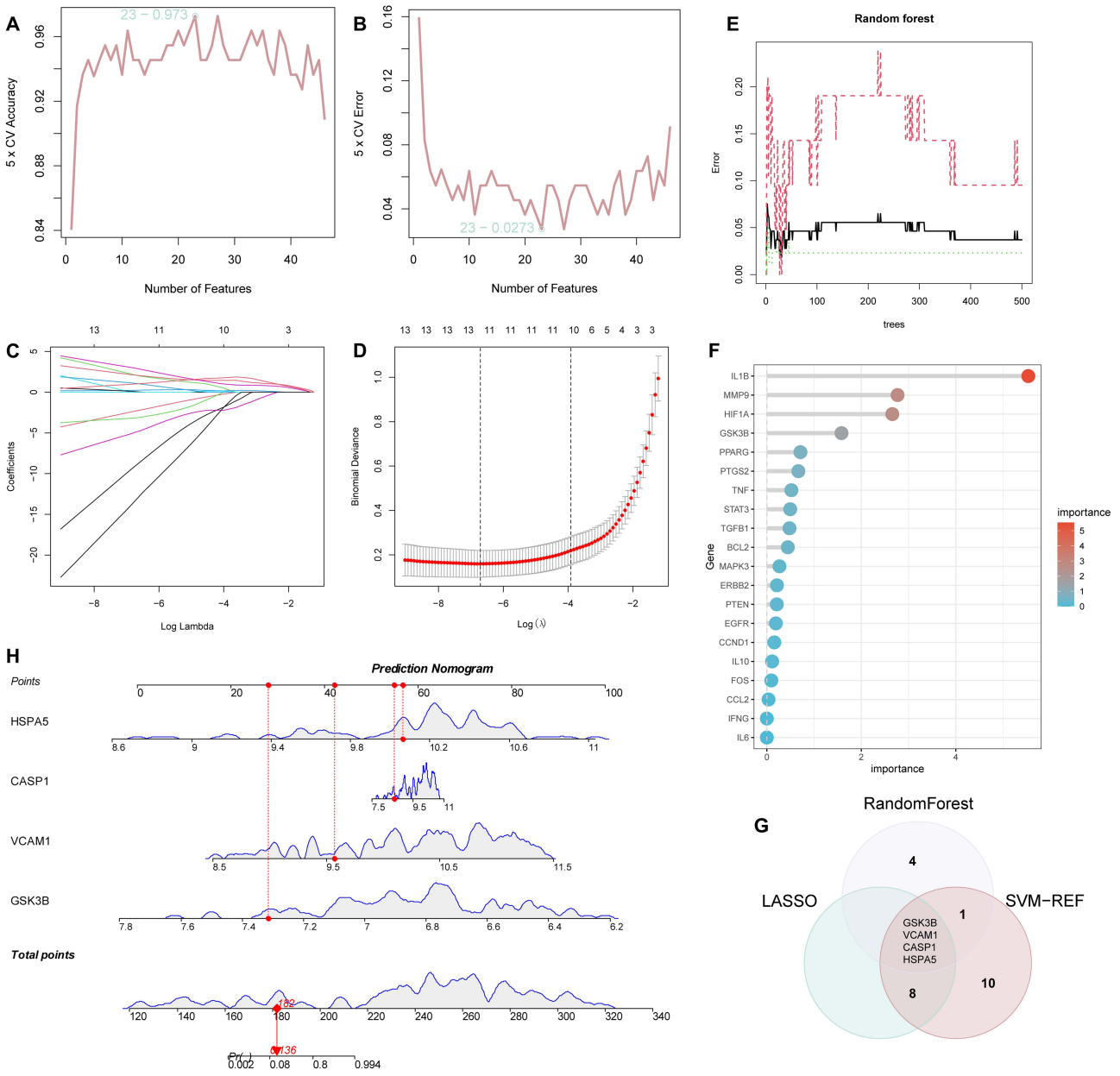

Figure 3 Analysis of machine learning models and construction of UC line diagram models. (**A** and **B**) Lasso regression analysis graph. (**C** and **D**) SVM-REF analysis graph. (**E** and **F**) Random forest analysis graph. (**G**) Intersection of the three machine learning results. (**H**) The column chart model of key target gene network graph.

In vitro Cellular Experiments

CCK-8 results showed that cell viability was largely unaffected by treatment of RAW264.7 with low, medium, or high doses of JJHF or mesalazine-containing serum compared to the blank group, suggesting that there was no cytotoxicity of the above administered doses on RAW264.7 (Figure 5A). Therefore, we next assessed the effect of JJHF on inflammatory cytokine production in LPS-stimulated RAW264.7 cell culture supernatants, and the results showed that the levels of IL-1β (Figure 5B), TNF-α (Figure 5C), and MCP-1 (Figure 5D) in the model group were significantly higher than in the blank group. On the contrary, low, medium, and high doses of JJHF treatment significantly reduced the levels of these cytokines, with the high dose group having levels comparable to those of the mesalazine group (Figure 5B–D). In order to confirm the accuracy of the key targets HSPA5, GSK3B, VCAM1 and CASP1 obtained by screening based on network pharmacology, machine learning, etc., we performed qRT-PCR analysis, which showed that after LPS stimulation and different serum treatments, the model group of HSPA5 (Figure 5E), VCAM1 (Figure 5F), GSK3B (Figure 5G) and

https://doi.org/10.2147/JIR.S527482

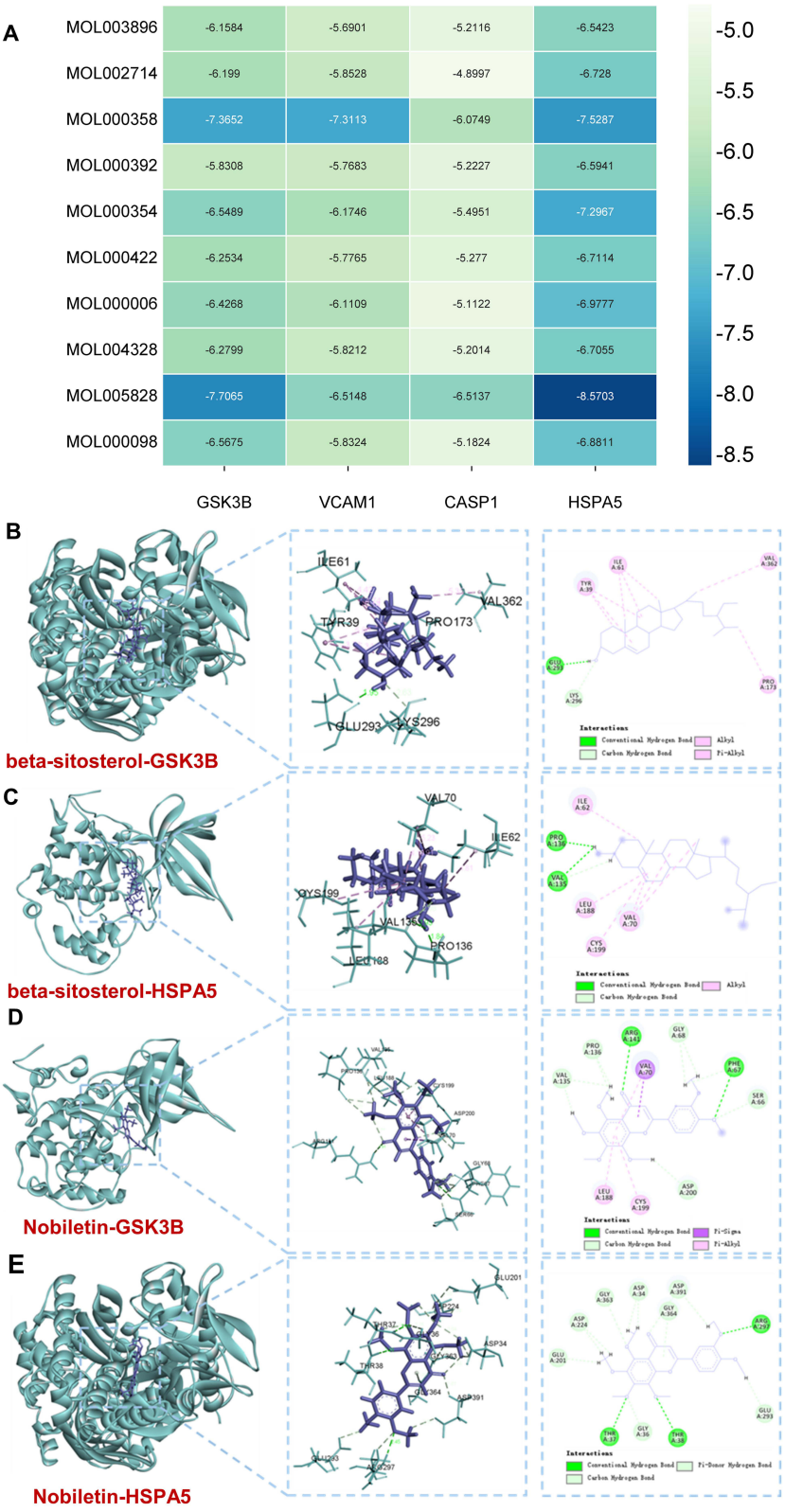

Figure 4 Molecular docking. (**A**) Diagram showing the binding energy of molecular docking results. (**B**–**E**) The molecular docking diagram of core components and key genes.

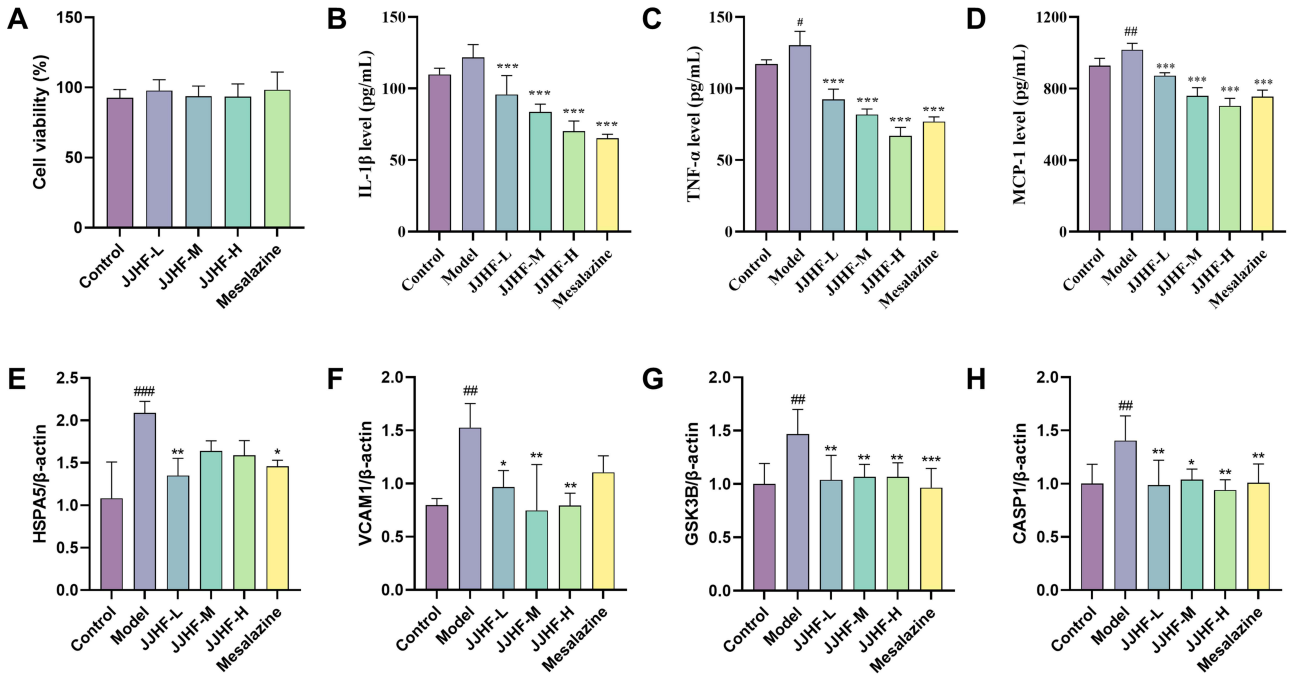

Figure 5 In vitro cellular experiments. (**A**) CCK-8 assay. (**B**–**D**) The expression level of IL-1β, TNF-α, and MCP-1 was detected by ELISA. (**E**–**H**) The mRNA expression of core target HSPA5, GSK3B, VCAM1 and CASP1 by qRT-PCR. $^{\#\#\#\#}p < 0.001$, $^{\#\#\#}p < 0.001$, $^{\#}p < 0.001$ vs the control group, $^{***}p < 0.001$, $^{**}p < 0.01$, $^{*}p < 0.05$ vs the model group. $p > 0.05$ vs the mesalazine group.

CASP1 (Figure 5H) mRNA expression was significantly higher than that of the blank group. Notably, compared with the model group, the gene expression levels of HSPA5, GSK3B, VCAM1 and CASP1 were down-regulated by low, medium and high doses of JJHF with different degrees of significance. The mRNA levels in the high-dose JJHF group were not significantly different from those in the mesalazine group, indicating that its regulatory effect on the expression of these genes was comparable to that of mesalazine (Figure 5E–H). In conclusion, the above results collectively showed that JJHF significantly reduced the production of pro-inflammatory cytokines and regulated the expression of core targets such as HSPA5, GSK3B, VCAM1, and CASP1 in the cells after LPS stimulation of RAW264.7. These results highlight the value of JJHF as a potential drug for the treatment of UC.

In vivo Animal Experimental Validation

To further evaluate the therapeutic effects of JJHF on UC in a mouse model, we conducted several in vivo experiments. We divided the experiments into a control group, a model group, and different treatment groups, which included high, medium, and low doses of JJHF as well as a mesalazine group (Figure 6A). Throughout the experiments, we monitored the changes in body weight of the mice in each group. The results showed a significant decrease in body weight in the model group compared with the control group. In contrast, treatment with JJHF significantly reduced weight loss in a dose-dependent manner, with the most pronounced improvement in the high-dose group (Figure 6B). We also evaluated the DAI scores, which were significantly elevated in the model group, indicating severe disease activity. JJHF treatment led to a marked reduction in DAI scores across all treatment groups, especially in the high-dose JJHF and mesalazine groups, bringing them closer to control levels (Figure 6C). Colon length, an important measure of colonic inflammation, was significantly reduced in the model group compared to the control group. Notably, administration of JJHF (especially at high doses) restored colon length to a level comparable to that of the mesalazine group when compared to the model group (Figure 6D and E). Fecal occult blood analysis showed a significant increase in positive results in the model group compared with the blank group, suggesting mucosal damage. JJHF treatment reduced the incidence of positive fecal occult blood test results in a dose-dependent manner, which was similar to the effect of mesalazine (Figure 6F). Histological examination using H&E staining revealed significant inflammatory changes characterized by crypt shedding

https://doi.org/10.2147/JIR.S527482

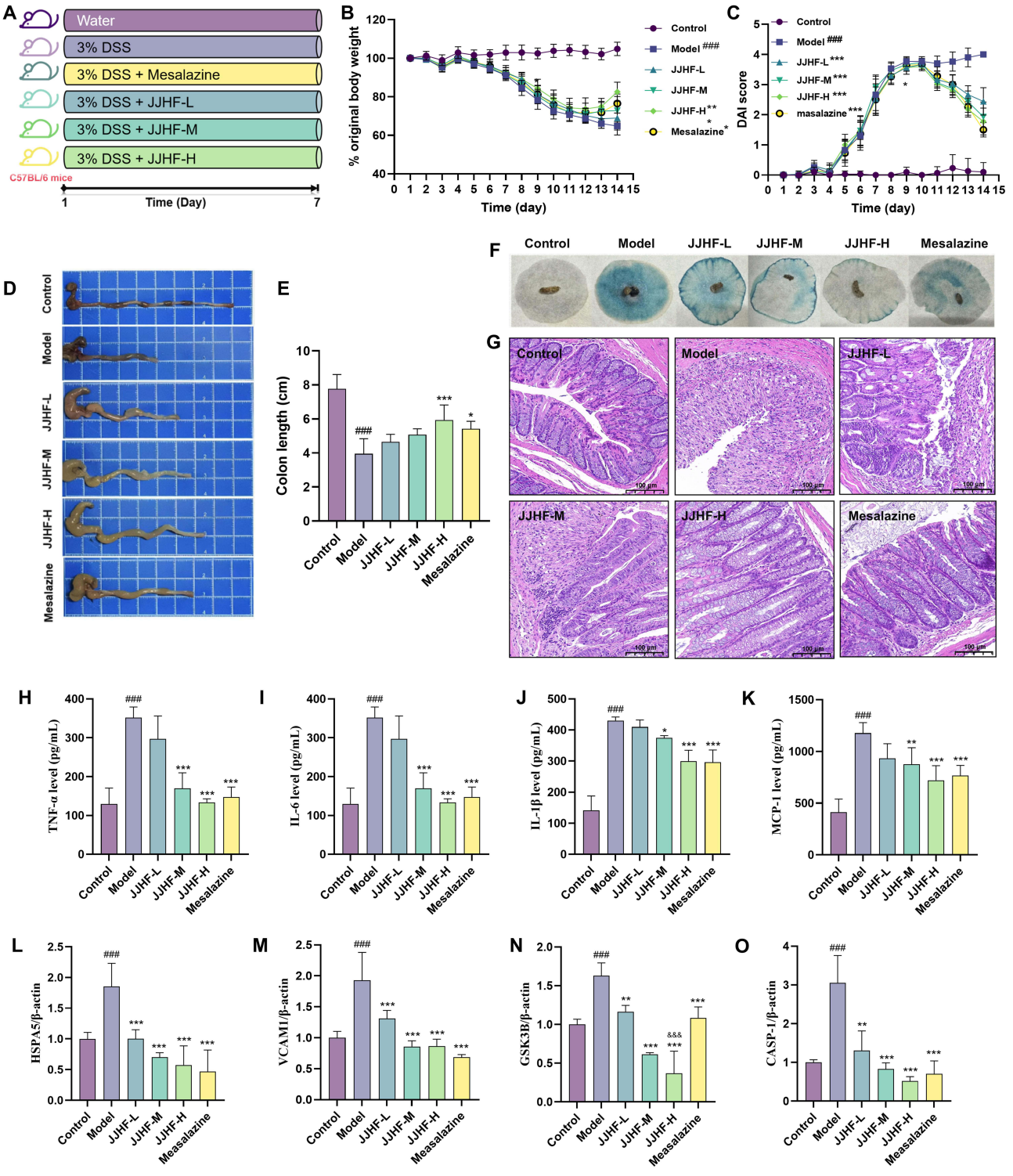

Figure 6 In vivo experimental validation. (**A**) Experimental design flow chart. (**B**) The body weight changes of mice in each group. (**C**) Disease activity index (DAI) scores. (**D**) Typical images comparing the length of the colon in each group. (**E**) The colon length of mice in each group. (**F**) Observation of fecal occult blood in each group. (**G**) Representative images for H&E staining of colon cross-sections (Scale = 100 μm). (**H**–**K**) The expression level of TNF-α, IL-6, IL-1β, and MCP-1 in colon tissues was detected by ELISA. (**L**–**O**) The mRNA expression of core target HSPA5, VCAM1 GSK3B, and CASP1 in colon tissues by qRT-PCR. $^{\#\#\#}p < 0.001$ vs the control group, $^{***}p < 0.001$, $^{**}p < 0.01$, $^{*}p < 0.05$ vs the model group. $p > 0.05$, $^{\&\&\&}p < 0.001$ vs the mesalazine group.

and inflammatory cell infiltration in the model group compared to the blank group. In comparison with the model group, the JJHF-treated group showed reduced inflammation and better protection of colonic structures, especially in the high-dose cohort (Figure 6G). We also measured the levels of pro-inflammatory cytokines and found that the model group had significantly higher levels of TNF-α, IL-6, IL-1β and MCP-1 compared to the blank group. In contrast, JJHF treatment was able to significantly reduce the levels of these cytokines compared with the model group, with the greatest reduction in the high-dose group, which was close to the levels of the control group (Figure 6H–K). In addition, we analyzed the mRNA expression of 4 key inflammatory mediators and stress markers (including HSPA5, VCAM1, GSK3B, and CASP1) obtained by bioinformatics screening using qRT-PCR (Figure 6L–O). It was found that the model group showed increased expression of these genes compared with the control group, whereas JJHF treatment effectively reduced their expression, especially in the high-dose group. Compared with the mesalazine group, except for GSK3B, which showed significant differences, there were no significant differences in other indicators. This suggests that JJHF is comparable to or even superior to mesalazine in efficacy. Overall, these findings demonstrated a better anti-inflammatory effect of JJHF in the UC mouse model, while HSPA5, VCAM1, GSK3B and CASP1 may play important roles in this process.

Mendelian Randomization (MR) Analysis of the Relationship Between Key Genes and UC

We utilized the MR analysis method to investigate the complex relationship between key genes and UC, determining whether their relationship is causal or merely correlational. By employing machine learning algorithms and the IEU database, we obtained information on SNPs of two key genes (GSK3B and HSPA5), as SNPs related to VCAM1 and CASP1 were not found and thus not included in this analysis. None of the SNPs were weak IVs (Figure 7A). Subsequently, we delved into the causal effects of these two key genes on the progression of UC. Following Bonferroni correction ($p=0.05/5$), we proceeded with IVW analysis. This analysis revealed a positive correlation between the expression level of the HSPA5 gene and the risk of UC, meaning that a higher level of HSPA5 corresponds to a higher risk of UC. Specifically, the OR value was 5.639 (95% CI range 1.085–29.306), with a P value of 0.040, indicating a significant association between increased HSPA5 levels and the risk of UC disease. In contrast, there was no significant causal relationship between GSK3B and UC (Figure 7A). The IVW analysis for HSPA5's causal impact on UC is shown in Figure 7B and E. The causal effect funnel plot is approximately symmetrical (Figure 7C). After conducting leave-one-out analysis, consistent results were observed in MR analysis even when individual SNPs were removed and the remaining SNPs were analyzed (Figure 7D), emphasizing the robustness of this finding. No heterogeneity was detected in the results for HSPA5 using Cochran's Q test ($p>0.05$). MR-Egger regression and MR-PRESSO analysis showed no evidence of horizontal pleiotropy in the results for HSPA5 ($p>0.05$).

Discussion

In this study, we elucidated the therapeutic potential of JJHF in treating UC through a comprehensive multi-strategies and pharmacological exploration. By integrating network pharmacology, machine learning, molecular docking, MR analysis and experimental validation, we have identified key active ingredients and molecular targets through which JJHF exerts its effects on UC. These findings have important translational medicine potential. First, unlike single-target biologics commonly used in the treatment of UC, the multi-target regulatory mechanism of JJHF significantly reduces the risk of drug resistance development, which is a long-term challenge in the management of UC. This multi-component, multi-target strategy also implies its broader efficacy in different UC subtypes due to its ability to act simultaneously on multiple pathological pathways, including those related to spleen deficiency, blood stasis, and inflammation. This feature not only enhances the potential therapeutic benefit, but also expands the clinical applicability of JJHF, providing a novel and promising alternative for personalized treatment. Second, the identified key components and targets could serve as the basis for the development of standardized JJHF-based formulations with well-defined therapeutic properties, which could accelerate the drug development process for UC. Third, the safety and efficacy of JJHF demonstrated in preclinical models provide a solid basis for initiating clinical trials to evaluate its efficacy in human patients. Fourth, the multidimensional pharmacodynamic properties revealed by JJHF provide new insights into precision medicine strategies for UC that hold promise for personalized treatment by targeting specific pathways perturbed in the disease phenotype of individual patients. These insights not only highlight the possibility of

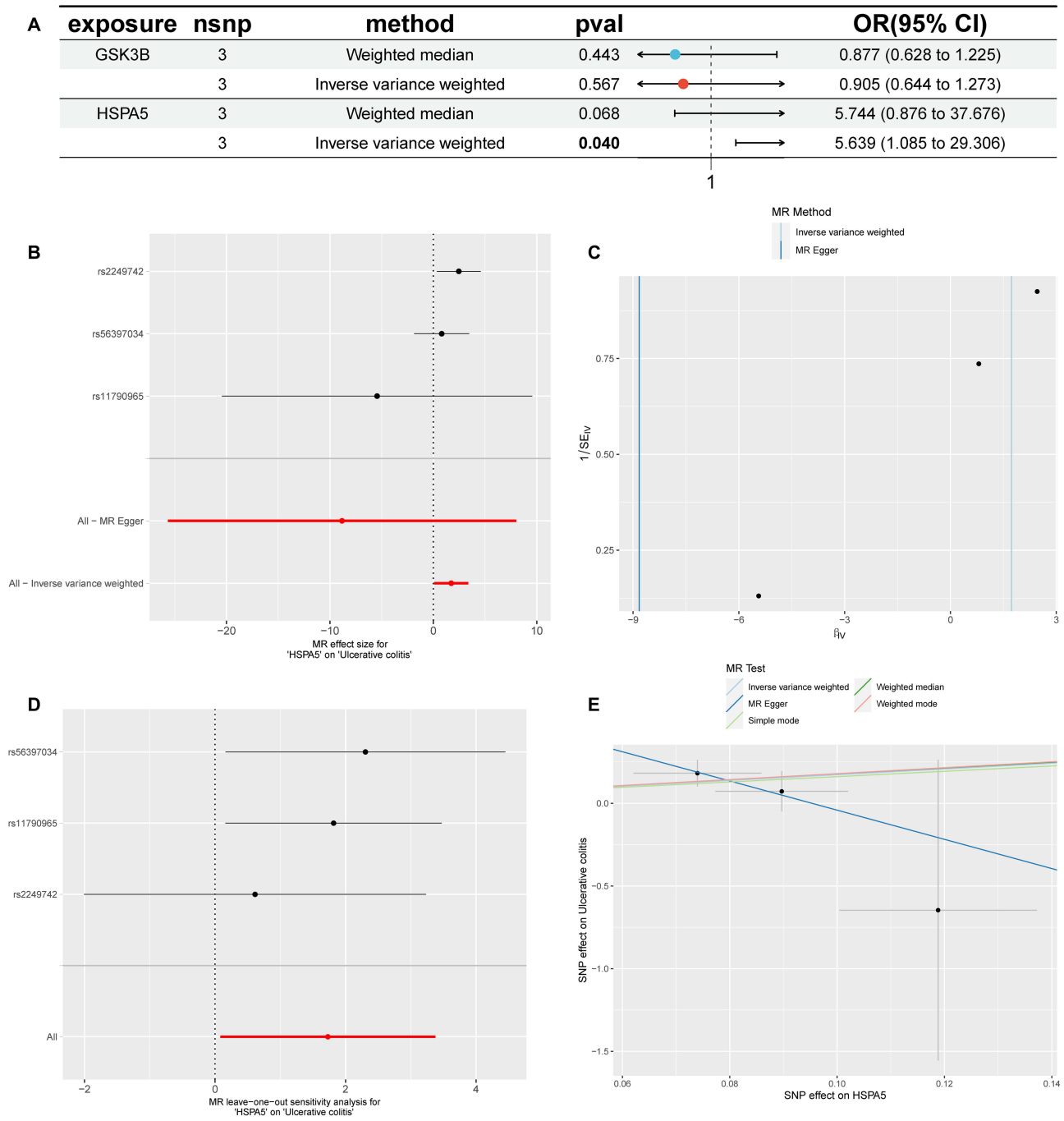

Figure 7 MR analysis of the relationship between key genes and UC. (**A**) Forest plot showing the causal relationship between two key genes and UC under the IVW method. (**B**) Impact of each SNP in HSPA5 on the risk of UC. (**C**) Funnel plot of HSPA5 on UC. (**D**) Omission plot of HSPA5 on UC risk when leaving one SNP. (**E**) Scatter plot of the causal relationship between HSPA5 and UC risk.

JJHF as a potential UC therapeutic drug, which not only promotes the application of JJHF in the clinic, but also provides a scientific basis for its in-depth mechanistic studies in later stages.

Our "drug-component-target-disease" network analysis underscores the complexity of JJHF's interactions, revealing a multi-component, multi-target, and multi-pathway approach to UC treatment. Notably, Quercetin, luteolin, and kaempferol stood out among the identified compounds because of their significant connectivity in our drug-disease network. A study demonstrated that quercetin enhances the integrity of tight junctions in an AhR-dependent way, thereby easing colitis in mice. Further in vitro studies revealed that quercetin enhances the expression of tight junction proteins

and activates AhR in a dose-dependent way, shedding light on its role in improving intestinal barrier function.[17] Moreover, it was demonstrated that quercetin can suppress the inflammatory response triggered by LPS in healthy organ tissues and also the spontaneous inflammation in UC organ tissues.[18] Moreover, lignans were discovered to enhance the function of the intestinal epithelial barrier by boosting the expression of resistance and tight junction proteins. This resulted in the reduction of DSS-induced UC in mice by blocking the STAT3 pathway through SHP-1.[19] Luteolin may alleviate DSS-induced colitis in rats, and gut microbiota could serve as promising biomarkers to comprehend how luteolin enhances UC.[20] Additionally, studies suggest that kaempferol aids in reducing experimental colitis in mice by regulating gut microbiota and obstructing the LPS/TLR4/NF-κB pathway.[21] Overall, this study backs the comprehensive approach of TCM, suggesting that therapeutic benefits come from the combined actions of various components. The discovery of highly interconnected compounds in our drug-disease network indicates that these elements are crucial in influencing the pathological process of UC. PPI network analysis underscored the critical role of inflammatory pathways, with key cytokines such as TNF, IL6, and IL1β serving as major intermediary nodes, demonstrating JJHF's ability to affect immune and inflammatory responses.

Further, using machine learning, we identified four targets (including GSK3B, VCAM1, CASP1 and HSPA5) that may play crucial roles in the pathophysiological processes associated with UC. Some findings suggest that carbon monoxide attenuates DSS-induced colitis by inhibiting GSK-3β signaling in vitro and in vivo, which is the first report of this molecular mechanism in this model of colitis.[22] CASP1 and HSPA5 have also been demonstrated as core targets of UC in some studies as well.[23,24] Molecular docking analyses offered important insights into the interactions between the key active components of JJHF and their target proteins. The strong binding affinities observed, particularly between beta-sitosterol and HSPA5, provide a molecular foundation for the therapeutic effects noted in our studies. This enhances our understanding of the bioactivity at a structural level, illustrating how these compounds may exert their beneficial actions. The MR analysis unveiled a significant causal relationship between elevated HSPA5 levels and increased UC risk, emphasizing HSPA5 as a potential therapeutic target for JJHF.

Our immune infiltration analysis distinguished notable differences in immune cell compositions between UC patients and healthy controls. Specifically, the upregulation of pro-inflammatory immune cells such as T cells gamma delta and macrophages M1 in UC samples aligns with JJHF's observed modulation of inflammatory cytokines in vitro. The suppression of IL-1β, TNF-α, and MCP-1 in LPS-stimulated RAW264.7 cells highlights JJHF's ability to attenuate inflammatory responses, presumably through its action on key molecular targets and pathways identified in our analyses. Furthermore, the machine learning models identified GSK3B, VCAM1, CASP1, and HSPA5 as crucial diagnostic markers for UC. In vitro and in vivo experiments further demonstrated the potential of JJHF for the treatment of UC by down-regulating key inflammatory genes (GSK3B, VCAM1, CASP1 and HSPA5) and thus affecting the signalling pathways involved in the pathological process of UC. The absence of cytotoxicity at different doses of JJHF confirms the safety of JJHF and lays the foundation for its clinical application. It is worth noting that in our animal studies, we found that low, medium, and high doses of JJHF all had certain therapeutic effects on UC. The medium and high doses of JJHF were basically equivalent to mesalazine, while the high dose of JJHF was even more effective. Although our current study provides insights for the subsequent study of JJHF, there are some limitations. First, our entire study was only a preliminary validation of potency and target of action through cellular and animal experiments, which cannot fully reflect the complex dynamics of JJHF in treating UC. Therefore, subsequent in-depth mechanistic studies based on cellular and animal models are essential to confirm these predictions. Additionally, the lack of comprehensive chemical profiling for key compounds (eg, quercetin) may impact batch-to-batch reproducibility of JJHF, despite sourcing materials compliant with pharmacopoeial standards. In terms of genetics, the findings are consistent with existing theories, which all emphasise the important role of genetic factors in the pathogenesis of UC. However, single nucleotide polymorphisms (SNPs) in certain key genes (eg, VCAM1 and CASP1) were missing and could not be included in the final analyses, which may affect the comprehensiveness of the study. Moreover, single-cell sequencing data would enable a more detailed dissection of the immune microenvironment, allowing for the identification of rare cell populations and the elucidation of cell-cell interactions at a single-cell level. Due to resource constraints and the specific focus of our current study, we were unable to incorporate this advanced technique. Additionally, our study did not explore the effects of JJHF on the gut microbiota or the dynamic interactions between JJHF and gut bacterial communities, which may

influence the therapeutic efficacy of JJHF. The gut microbiota plays a key role in the pathogenesis of UC. Investigating how JJHF modulates the composition and function of microbial communities may provide deeper insights into its mechanisms. Future studies should focus on collecting and analysing associations of more key genes more comprehensively and validating our findings in different populations and geographic regions, and conducting in-depth investigations into the impact of JJHF on gut microbiota through approaches such as 16S rRNA sequencing and fecal microbiota transplantation. As well as conducting in-depth exploration of the HSPA5-ER stress pathway via targeted knockout/rescue experiments. In addition, an in-depth exploration of the specific biological mechanisms between increased HSPA5 expression and increased risk of UC will be an important direction for future research.

Conclusion

In this study, we found that quercetin, lignans and kaempferol play an important role in the therapeutic efficacy of UC and are the key active ingredients of JJHF for the treatment of UC. Using machine learning techniques, we identified key genes such as GSK3B, VCAM1, CASP1, and HSPA5, which were further validated by molecular docking studies, thus confirming their strong molecular interactions. The therapeutic potential of JJHF was further confirmed by the significant reduction of inflammatory cytokines (TNF, IL6, and IL1β) and modulation of the expression of key genes (GSK3B, VCAM1, CASP1, and HSPA5) in LPS-stimulated RAW264.7 cells and 3% DSS-induced mouse UC model. Notably, in the correlation analysis between HSPA5 expression and UC risk, we found a potential causal link between them, which provides more insight into the pathological mechanisms of UC. From a clinical perspective, the identified active ingredients and key genes suggest that JJHF may offer a novel therapeutic strategy for UC. Future research could focus on conducting pre-clinical toxicology studies to evaluate the safety of JJHF, and then progressing to well-designed human clinical trials to validate its efficacy and optimal dosing regimens. Moreover, investigating the combined effects of the key active components in JJHF could provide greater insights into its therapeutic mechanisms, potentially leading to the development of more targeted and effective treatments for UC. In conclusion, these findings not only provide a reliable basis for the application of JJHF in the treatment of UC, but also provide a target reference and methodological reference for the use of other compounding agents in UC treatment.

Data Sharing Statement

Data is contained within the article and Supplementary Materials.

Ethics Approval and Consent to Participate

The animal experiment procedure was carried out in strict accordance with the National Institutes of Health Guide for the Care and Use of Laboratory Animals and approved by the animal ethics committee of the experimental animal center of Henan University of Traditional Chinese Medicine (Approval No.: 202312043). In addition, the GeneCards, CTD, and GEO are public databases whose data contributors have provided prior ethical consent for research use. Researchers may freely utilize these resources for data acquisition and subsequent publication. So, the animal ethics committee of the experimental animal center of Henan University of Traditional Chinese Medicine has formally waived ethical approval requirements for this study.

Author Contributions

All authors made a significant contribution to the work reported, whether that is in the conception, study design, execution, acquisition of data, analysis and interpretation, or in all these areas; took part in drafting, revising or critically reviewing the article; gave final approval of the version to be published; have agreed on the journal to which the article has been submitted; and agree to be accountable for all aspects of the work.

Funding

This study was supported by the "Zhang Zhongjing Inheritance and Innovation Special Project" (GZY-KJS-2022-044-1) from the Science and Technology Department of the National Administration of Traditional Chinese Medicine; the Key Project of Henan Province Science and Technology Research and Development Program Joint Fund (222301420021); the Joint Fund of Science and Technology Research and Development Plan of Henan Province (222301420023); and the Scientific and Technological Innovation Teams of Colleges and Universities in Henan Province (23IRTSTHN028).

Disclosure

The authors declare no conflicts of interest in this work.

References

1. Kobayashi T, Siegmund B, Le Berre C, et al. Ulcerative colitis. *Nat Rev Dis Primers*. 2020;6(1):74. doi:10.1038/s41572-020-0205-x
2. Le Berre C, Honap S, Peyrin-Biroulet L. Ulcerative colitis. *Lancet*. 2023;402(10401):571–584. doi:10.1016/s0140-6736(23)00966-2
3. Nakase H, Sato N, Mizuno N, Ikawa Y. The influence of cytokines on the complex pathology of ulcerative colitis. *Autoimmunity Rev*. 2022;21(3):103017. doi:10.1016/j.autrev.2021.103017
4. Gravina AG, Panarese I, Trotta MC, et al. Melanocortin 3,5 receptors immunohistochemical expression in colonic mucosa of inflammatory bowel disease patients: a matter of disease activity? *World J Gastroenterol*. 2024;30(9):1132–1142. doi:10.3748/wjg.v30.i9.1132
5. Liu L, Lu C, Tao Z, Zha Z, Wang H, Miao Z. 2D is better: engineering polydopamine into cationic nanosheets to enhance anti-inflammatory capability. *Adv Healthcare Mater*. 2024;13(18):e2400048. doi:10.1002/adhm.202400048
6. Li R, Fan Y, Liu L, et al. Ultrathin hafnium disulfide atomic crystals with ROS-scavenging and colon-targeting capabilities for inflammatory bowel disease treatment. *ACS Nano*. 2022;16(9):15026–15041. doi:10.1021/acsnano.2c06151
7. Feuerstein JD, Moss AC, Farraye FA. Ulcerative Colitis. *Mayo Clin Proc*. 2019;94(7):1357–1373. doi:10.1016/j.mayocp.2019.01.018
8. Kim HJ, Eom JY, Choi SH, et al. Plum prevents intestinal and hepatic inflammation in the acute and chronic models of dextran sulfate sodium-induced mouse colitis. *Mol Nutr Food Res*. 2022;66(13):e2101049. doi:10.1002/mnfr.202101049
9. Zheng S, Xue T, Wang B, Guo H, Liu Q. Chinese medicine in the treatment of ulcerative colitis: the mechanisms of signaling pathway regulations. *Am J Chin Med*. 2022;50(7):1781–1798. doi:10.1142/s0192415x22500756
10. Liu Y, Li BG, Su YH, et al. Potential activity of Traditional Chinese Medicine against ulcerative colitis: a review. *J Ethnopharmacol*. 2022;289:115084. doi:10.1016/j.jep.2022.115084
11. Lee M, Shin H, Park M, Kim A, Cha S, Lee H. Systems pharmacology approaches in herbal medicine research: a brief review. *BMB Rep*. 2022;55(9):417–428. doi:10.5483/BMBRep.2022.55.9.102
12. Zhao L, Zhang H, Li N, et al. Network pharmacology, a promising approach to reveal the pharmacology mechanism of Chinese medicine formula. *J Ethnopharmacol*. 2023;309:116306. doi:10.1016/j.jep.2023.116306
13. Su M, Zhu J, Bai L, Cao Y, Wang S. Exploring manzamine a: a promising anti-lung cancer agent from marine sponge Haliclona sp. *Front Pharmacol*. 2025;16:1525210. doi:10.3389/fphar.2025.1525210
14. Larsson SC, Butterworth AS, Burgess S. Mendelian randomization for cardiovascular diseases: principles and applications. *Eur Heart J*. 2023;44(47):4913–4924. doi:10.1093/eurheartj/ehad736
15. Chen LG, Tubbs JD, Liu Z, Thach TQ, Sham PC. Mendelian randomization: causal inference leveraging genetic data. *Psychol Med*. 2024;54(8):1461–1474. doi:10.1017/s0033291724000321
16. Huang J, Wang L, Zhou J, et al. Unveiling the ageing-related genes in diagnosing osteoarthritis with metabolic syndrome by integrated bioinformatics analysis and machine learning. *Artif Cells Nanomed Biotechnol*. 2025;53(1):57–68. doi:10.1080/21691401.2025.2471762
17. Wang X, Xie X, Li Y, et al. Quercetin ameliorates ulcerative colitis by activating aryl hydrocarbon receptor to improve intestinal barrier integrity. *Phytother Res*. 2024;38(1):253–264. doi:10.1002/ptr.8027
18. Dicarlo M, Teti G, Verna G, et al. Quercetin exposure suppresses the inflammatory pathway in intestinal organoids from winnie mice. *Int J Mol Sci*. 2019;20(22):5771. doi:10.3390/ijms20225771
19. Li BL, Zhao DY, Du PL, Wang XT, Yang Q, Cai YR. Luteolin alleviates ulcerative colitis through SHP-1/STAT3 pathway. *Inflammation Res*. 2021;70(6):705–717. doi:10.1007/s00011-021-01468-9
20. Li B, Du P, Du Y, et al. Luteolin alleviates inflammation and modulates gut microbiota in ulcerative colitis rats. *Life Sci*. 2021;269:119008. doi:10.1016/j.lfs.2020.119008
21. Qu Y, Li X, Xu F, et al. Kaempferol alleviates murine experimental colitis by restoring gut microbiota and inhibiting the LPS-TLR4-NF-κB axis. *Front Immunol*. 2021;12:679897. doi:10.3389/fimmu.2021.679897
22. Uddin MJ, Jeong SO, Zheng M, et al. Carbon monoxide attenuates dextran sulfate sodium-induced colitis via inhibition of GSK-3β signaling. *Oxid Med Cell Longev*. 2013;2013:210563. doi:10.1155/2013/210563
23. Zhao Y, Ma Y, Pei J, Zhao X, Jiang Y, Liu Q. Exploring pyroptosis-related signature genes and potential drugs in ulcerative colitis by transcriptome data and animal experimental validation. *Inflammation*. 2024;47(6):2057–2076. doi:10.1007/s10753-024-02025-2
24. Gong ZZ, Li T, Yan H, et al. Exploring the autophagy-related pathogenesis of active ulcerative colitis. *World J Clin Cases*. 2024;12(9):1622–1633. doi:10.12998/wjcc.v12.i9.1622